Design Verification of Power Electronics Systems Subject to Bounded Uncertain Inputs

Eric M. Hope
Department of Electrical and Computer Engineering
University of Illinois at Urbana-Champaign
Urbana, IL 61801
Email: ehope2@illinois.edu

Alejandro D. Domínguez-García
Department of Electrical and Computer Engineering
University of Illinois at Urbana-Champaign
Urbana, IL 61801
Email: aledan@illinois.edu

Abstract—**A method for design verification of power electronics systems is proposed. In this method, the system is described by a linear switched state-space representation, where some or all of the inputs may vary without control over some bounded range, e.g., load current and input voltage. The method relies on solving the reachability problem associated with this system, which is the computation of the set of all possible trajectories that arise from different initial conditions, uncontrolled inputs, and inherent switching. The method allows one to verify whether or not this set (called the reach set) remains within a region of the state-space defined by performance requirements, e.g., output voltage tolerance. Algorithms to solve the reachability problem for power electronics converters with both open- and closed-loop control are provided. The application of the method is illustrated in buck and boost converter examples.**

I. INTRODUCTION

The operation of many power electronics systems is subject to uncertainty. This uncertainty can be classified into *operational uncertainty* and *structural uncertainty*. Operational uncertainty is usually associated with uncontrolled changes on the demand or the supply side. For example, in the buck converter of Fig. 1, the current demanded by the load is not fixed but can change over time in an uncontrolled manner, and therefore this is regarded as operational uncertainty. Structural uncertainty is associated with undesired changes in the physical structure of the system. In the buck converter of Fig. 1, a random fault in one component may be regarded as structural uncertainty.

During the design stage of a power electronics system, in order to verify the design against the performance requirements, it is necessary to carry out an extensive analysis to ensure the system behaves as expected for all possible operational conditions that arise due to operational and structural uncertainty. For example, the power supply specifications for the Intel® Pentium® 4 class of microprocessors require an extremely strict voltage regulation (± 25mV from the defined load line) over the entire range of current (0A to 70A) capable of being drawn by the processor [1]. This design requirement is enforced for both static and transient operation of the power supply, which means that these bounds cannot be violated for any load or any step change in the load. In addition, the source feeding the supply is allowed to vary within +5% and -8% of 12V [1]. Violating these voltage regulation requirements may

result in damage to or even failure of the microprocessor. The analysis required to verify the design against the requirements under such levels of uncertainty may seem overwhelming.

This analysis is usually conducted through time-domain simulations, where for each particular operational condition, a simulation is conducted to ensure the system behaves as expected [2], [3]. For example, in [3], Monte Carlo analysis is used to determine the effects of variations in component parameters (structural uncertainty) on system reliability. Depending on the size of the system and the different operational conditions, this simulation-based approach can be a daunting task.

This paper focuses on providing an analytically tractable method to quantify the effect of operational uncertainty on the behavior of power electronics systems. In this method, the system is described by a linear switched state-space representation, where some or all of the inputs may vary without control over some range, e.g., load current and input voltage. The method relies on solving the reachability problem associated with this linear switched system, which is *the computation of the set of possible trajectories that arise from different initial conditions, uncontrolled inputs, and inherent switching.* The method can be used to verify the converter design in nominal conditions.

This problem was addressed before in [4], where the reachability problem was formulated in terms of the linearized averaged model of the converter, without including the switching effects of the converter. Furthermore, the proposed solution to the reachability problem relied on the calculation of a bounding ellipsoid, which does not provide an exact solution. In this paper, both of these problems are solved by: 1) formulating the reachability problem in terms of the large-signal model of the converter (including switching); 2) providing a method to compute the exact solution to the reachability problem rather than providing an upper bound. Reachability methods recently proposed by Kurzhanski and Varaiya [5], [6] are adapted to the particular problem of power electronics system design verification. These methods provide an exact solution to the reachability problem using ellipsoidal calculus, ideas introduced by Schweppe and others (see, e.g., [7], [8], [9] and the references therein). Algorithms for addressing the verification of both open- and closed-loop
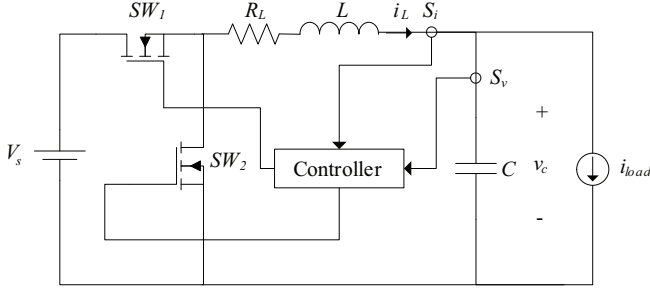
Fig. 1. Buck converter architecture.

controlled power electronics systems are provided.

A rough comparison of the simulation-based method to the proposed method is as follows. Considering only operational uncertainty, for each operational condition, with the simulation-based method, it would be necessary to solve n differential equations. Thus, if there are k operational conditions, it would be necessary to solve n differential equations k times. With the proposed method, it is only necessary to solve $n(n+1)/2+1$ differential equations to account for all possible operational conditions. Thus, for a small number of operational conditions, the simulation-based method may perform better. However, for large number of operational conditions (which is usually the case), the proposed method could provide an improvement over the simulation-based method.

The remainder of this paper is organized as follows. Section II presents the detailed mathematical formulation of the methodology for solving the reachability problem for power electronics systems, including systems operating with both open- and closed-loop control. In Sections III and IV, application examples of the methodology as applied to a buck and a boost converter respectively are presented. Concluding remarks are discussed in Section V.

II. MATHEMATICAL FORMULATION

The dynamics of a power electronics converter can be described, in general, by a linear switched state-space model of the form

$$\dot{x} = A_\sigma x + B_\sigma w, \qquad (1)$$

where $x \in \mathbb{R}^n$ represents the converter state variables, $w \in \mathbb{R}^p$ represents the uncontrolled input to the converter, the function $\sigma : [0, \infty) \rightarrow \mathcal{Q}$, called the switching signal, indicates the active converter configuration at every time, $\mathcal{Q}$ is called the "index set", and A_q and B_q with $q \in \mathcal{Q}$ define the matrices describing the converter dynamics for each switch configuration.

An unknown-but-bounded uncertainty model for the converter input w, in which $w \in \Omega_w$, where Ω_w is an arbitrary-shaped set, is assumed [7]. For computational simplicity, Ω_w is selected to be an ellipsoid that completely encloses the set of all possible inputs. This simplification will produce a solution that is an upper bound to the exact set of reachable states, unless the set of all possible inputs is an ellipsoid. Thus, Ω_w

is defined by

$$\Omega_w = \left\{ w : (w - w_c)'Q^{-1}(w - w_c) \le 1 \right\}, \qquad (2)$$

where w_c is a vector in $\mathbb{R}^n$ that defines the center of the ellipsoid Ω_w and $Q \in \mathbb{M}^{p \times p}$ is positive definite. For example, the uncontrolled inputs to the buck converter of Fig. 1 are the source voltage V_s and the load current i_{load}. In this case $w = [V_s\ i_{load}]'$. The inputs may have some uncontrolled variability defined by

$$|V_s - V_c| \le V, \quad |i_{load} - I_c| \le I, \qquad (3)$$

where V and I are positive constants, V_c is the dc value of the source voltage, and I_c is the nominal load current. Here, $w_c = [V_c\ I_c]'$ and Q is chosen such that Ω_w completely contains the set of all possible realizations of the inputs V_{in} and i_{out}. Figure 2 in Section III provides an illustration of this.

The problem is to obtain the so-called reach set, i.e., the set containing all possible converter trajectories, for all possible realizations over time of the uncontrolled inputs. This problem is known in the control literature as reachability. While there are many methods to solve the reachability problem (see e.g., [10], [11], [12], [13]) the ellipsoidal methods proposed in [5], [6] are adapted to the particular problem addressed in this paper, which is to obtain the reach set for the system in (1) given the input set defined by (2).

The reach set, denoted by $\mathcal{R}(t)$ can be obtained as the intersection of a family of ellipsoids:

$$\mathcal{R}(t) = \bigcap_\eta \mathcal{X}_\eta(t), \ \forall \eta \in \mathbb{R}^n \text{ such that } \eta'\eta = 1, \qquad (4)$$

with $\mathcal{X}_\eta = \{x : (x - x_c)'\Psi_\eta^{-1}(t)(x - x_c) \le 1\}$, where for each η, $\Psi_\eta(t)$ is obtained by solving

$$\frac{d\Psi_\eta(t)}{dt} = A_\sigma \Psi_\eta(t) + \Psi_\eta(t)A_\sigma' +$$
$$\beta_\eta(t)\Psi_\eta(t) + \frac{1}{\beta_\eta(t)}B_\sigma Q B_\sigma',$$

$$\beta_\eta(t) = \sqrt{\frac{\eta' e^{A_\sigma t}Q e^{A_\sigma' t}\eta}{\eta'\Psi_\eta(t)\eta}},$$
$$\Psi_\eta(0) = \Psi_0, \qquad (5)$$

where Ψ_0 is the same for all η and is chosen such that $\mathcal{R}(0)$ contains the set of all possible initial conditions, and x_c is defined by

$$\frac{dx_c}{dt} = A_\sigma x_c + B_\sigma w_c, \ x_c(0) = x_0. \qquad (6)$$

Next, the algorithm to obtain the solution to (5), which depends on the converter control strategy, will be presented.

A. Open-Loop Control

Open-loop control of power electronics converters is carried out by operating the switching devices at fixed intervals of time in order to achieve the desired output voltage(s) and/or current(s). For example, the switching function for a power electronics converter with m configurations (i.e. $q \in \mathcal{Q} = \{0, 1, \cdots, m-1\}$) could be given by

$$\sigma(t) = \begin{cases} 0, & kT \le t < (k+d_0)\,T \\ 1, & (k+d_0)\,T \le t < (k+d_0+d_1)\,T \\ ... \\ m-1, & \left(k + \sum\limits_{i=0}^{m-2} d_i\right) T \le t < (k+1)\,T, \quad (7) \end{cases}$$

where k is a nonnegative integer, T is the switching period, and d_i is the fraction of the switching period spent in the ith configuration. For a converter with only two configurations, d is typically referred to as the duty-ratio. The algorithm to obtain the reach set of a converter using the open-loop control specified in (7) is given by Algorithm 1, in which $\mathcal{R}(t)$ is computed in a piecewise manner from (4-6).

Algorithm 1 Open-loop reach set computation
___
start
  $\Psi_\eta(0) = \Psi_0$, $k = 0$
  repeat
    $\sigma = 0$
    compute $\mathcal{R}(t)$ for $t : [kT,\ kT + d_0 T)$
    for $\sigma = 1$ to $m-1$ **do**
      compute $\mathcal{R}(t)$ for $t : [kT + \sum\limits_{i=0}^{\sigma-1} d_i T,\ kT + \sum\limits_{i=0}^{\sigma} d_i T)$
    end for
    $k = k + 1$
  until $\mathcal{R}(t) = \mathcal{R}(t - T)$
end

This method assumes that the duty ratios remain constant over each switching period. However, the duty ratios are permitted to vary from switching period to switching period. Thus, this method may be applied to control schemes in which the values of d_i may vary over time, assuming these values change as a function of the switching period and this function is known. For example, a converter may have one set of d_i values during the startup period and another set of d_i values for steady-state operation.

B. Closed-Loop Control

Closed-loop control of power electronics converters is carried out by using state feedback to compute the value of the switching function. A general closed-loop control law for a power electronics converter is given by

$$\sigma(x,t) = f(x,t), \qquad (8)$$

where f is a function of the states of the converter and of time. The function f determines the switch actions required to drive the system to the desired operating point.

All closed-loop control laws of the form given in (8) may be described by some switching surface (or guard) G in the converter state space. Even if the controller has some dynamics, e.g., a PID controller, it can be shown that the closed-loop converter state-space description can be rewritten such that the converter closed-loop dynamics can be described

by (1) and (8), where x also includes the controller state variables. The position of the converter state variables in the state space in relation to the switching surface determines the necessary switch configuration. A switch action occurs when the state trajectory crosses the switching surface [14]. For example, a PWM controller for a converter with two possible switching configurations may have the form

$$\sigma(x,t) = u\left[K'\left(x_{ref} - x\right) + \Delta_{tri}(t)\right], \qquad (9)$$

where u is the Heaviside step function, x is a vector containing the converter state variables, x_{ref} is the desired system operating point, K is a gain vector, and $\Delta_{tri}(t)$ is a periodic triangle wave [14]. For this case, the switching surface is a linear surface that oscillates with time due to the periodic triangular wave component. This surface divides the state space into two regions. The region in which the converter state variables lie determines the active converter configuration.

For simplicity, the formulation is limited to converters with two possible switching configurations and a closed-loop control that uses only static (non-time varying) linear switching surfaces. In this case, the switching function is solely a function of the converter state variables:

$$\sigma(x) = u\left[K'\left(x_{ref} - x\right)\right]. \qquad (10)$$

The algorithm to obtain the reach set of a converter using the closed-loop control specified in (10) is given by Algorithm 2, in which a reach set $\mathcal{R}_k(t)$ is computed from (4-6), with initial condition specified by $\Psi_\eta(0)$, for each time interval k between successive switch actions. The union of all of these reach sets gives $\mathcal{R}(t)$ at the end of the algorithm.

Algorithm 2 Closed-loop reach set computation
___
start
  $\Psi_\eta(0) = \Psi_0$, $k = 0$
  compute σ from (10)
  repeat
    repeat
      compute $\mathcal{R}_k(t)$
      $\mathcal{Y}(t) = \mathcal{R}_k(t) \bigcap G$
    until $\mathcal{R}_k(t)$ completely passes through G
    compute σ from (10)
    pick $\Psi_\eta(0)$ such that $\mathcal{X}_\eta(0) \supseteq \mathcal{Y}(t)$
    $\mathcal{Y}(t) = \{\emptyset\}$
    $k = k + 1$
  until $\mathcal{R}_{k-2}(t) = \mathcal{R}_k(t)$ and $\mathcal{R}_{k-3}(t) = \mathcal{R}_{k-1}(t)$
  $\mathcal{R}(t) = \bigcup\limits_k \mathcal{R}_k(t)$
end

Some controllers may use multiple switching surfaces, and in other cases, devices within the circuit (e.g. diodes) introduce additional switching surfaces. An example of this is the discontinuous conduction mode of operation. The methodology presented here may be extended to multiple switching surfaces. This will be presented by example in Sections III and IV.

III. Buck Converter Analysis

Consider the buck converter of Fig. 1. In this section, the algorithms introduced in Section II will be applied to compute the converter reach set for both open- and closed-loop control. For a buck converter operating in continuous mode, i.e. $\mathcal{Q} = \{0, 1\}$,

$$A_0 = \begin{bmatrix} -\frac{R_L}{L} & -\frac{1}{L} \\ \frac{1}{C} & 0 \end{bmatrix}, \quad B_0 = \begin{bmatrix} 0 \\ -\frac{1}{C} \end{bmatrix},$$

$$A_1 = \begin{bmatrix} -\frac{R_L}{L} & -\frac{1}{L} \\ \frac{1}{C} & 0 \end{bmatrix}, \quad B_1 = \begin{bmatrix} 0 & \frac{1}{L} \\ -\frac{1}{C} & 0 \end{bmatrix}, \quad (11)$$

where $q = 1$ when SW_1 is closed and SW_2 is open and $q = 0$ when SW_1 is open and SW_2 is closed. As previously mentioned, the uncontrolled inputs to this converter are the source voltage V_s and the load current i_{load}.

Suppose there is a need to design a converter that has an uncertain voltage input and uncertain load as specified by (3). For example, the converter may have a variable load and may be supplied by a battery with some uncertain ripple. Let us also suppose that the design requires the output voltage be regulated with an acceptable tolerance specified by $|v_{out} - V_{out}| \leq \lambda V_{out}$, where V_{out} is the desired dc value of the output voltage.

A. Open-Loop Design Verification

Let us first consider the open-loop verification method as applied to the buck converter of Fig. 1, with parameters given in Table I. Equation (3) describes the bounds on the converter inputs. The function of this converter is to step down the 12V dc input to an output value of 5V dc. The input space is two-dimensional and the set of all possible realizations of the input is a rectangle. For computational simplicity, it was assumed that Ω_w is the minimum volume ellipsoid that encloses this rectangle. This assumption yields a solution that is an upper bound to the set of reachable states of the converter. See Fig. 2 for a graphical depiction of the input space for the input parameters given in Table I. In this figure the exact set of all possible inputs is contained within the blue rectangle and the minimum volume ellipsoid that encloses this rectangle is shown in red.
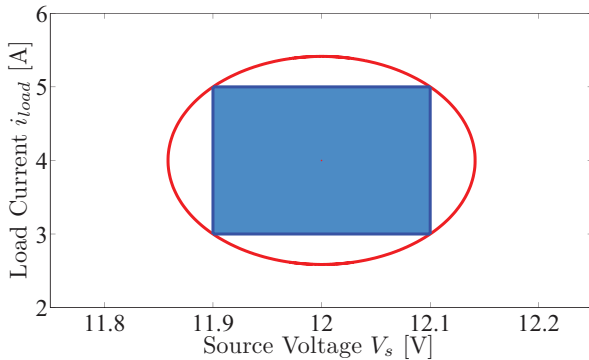
The switching function for this converter is given by

$$q(t) = \begin{cases} 0 & kT \leq t < (k + D)\, T \\ 1 & (k + D)\, T \leq t < (k + 1)\, T \end{cases} \quad (12)$$

TABLE I
OPEN-LOOP BUCK CONVERTER PARAMETERS

R_L [Ω]	0.1	V_c [V]	12
L [H]	12e-6	V [V]	0.1
C [F]	1.5e-3	I_c [A]	4
f [kHz]	250	I [A]	1
D	0.45	λ [%]	5

Equation (5) was solved, for $\eta_1 = [1\ 0]'$ and $\eta_2 = [0\ 1]'$, using the algorithm for solving the reachability problem of open-loop converters with the converter state-space matrices given in (11) and switching function given in (12), for a sufficiently long period of time to allow the reach set to come to a steady-state solution, i.e., $\mathcal{R}(t) = \mathcal{R}(t - T)$. Computation was performed using the Ellipsoidal Toolbox for MATLAB$^{\circledR}$ [15]. The open-loop reach set $\mathcal{R}(t)$ for the buck converter in steady-state operation is shown in Fig. 3. During steady-state operation, the reach set oscillates around some fixed point over the course of each switching period. Two sets of ellipsoids, one for each η (η_1 shown in blue and η_2 shown in red), are shown. The center points of the ellipsoids are shown by the blue dots. Each ellipsoid in the two sets shown give the solution to (5) at selected points in time during one switching period of the converter's steady-state operation. An upper bound to the set of reachable states for the open-loop buck converter at a given point in time is given by the intersection of the two ellipsoids (i.e. the ellipsoids for η_1 and η_2 at that point in time). The union of these intersections gives an upper bound to the set of reachable states over the entire switching period. Also shown in the figure, by the dotted black traces, is the output voltage tolerance as specified by the converter design requirements. It can be seen that the steady-state reach set for the open-loop converter remains within the acceptable voltage range for any possible realization of the input.
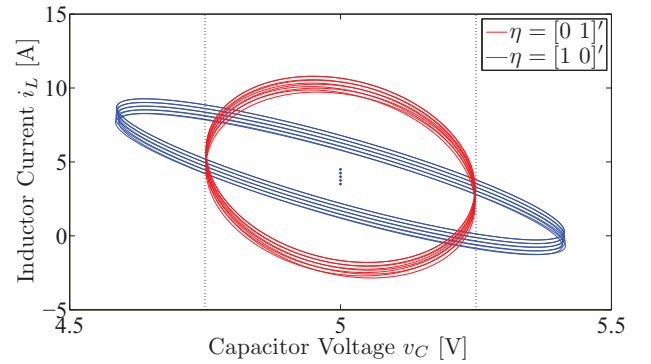

Fig. 2. Buck converter input space.

Fig. 3. Open-loop reach set for the buck converter of Table I.

B. Closed-Loop Design Verification

Next, the closed-loop verification method is illustrated by a buck converter that uses static linear switching boundary to control the switch actions in order to step down 12V dc to 5V dc. A linear switching boundary is given by (10). In the case of the buck converter, $K = [k_i \ k_v]'$ and $x_{ref} = [I_{ref} \ V_{ref}]'$, where I_{ref} is the desired inductor current, V_{ref} is the desired output voltage at nominal current, k_i is the current gain and k_v is the voltage gain. It was assumed for this case that the input voltage is fixed and not subject to uncertain variations.

Here, the converter architecture was modified such that SW_2 is implemented by a diode. The diode will block negative current from passing through SW_2 and thus a third switching configuration (SW_1 and SW_2 both open) is possible for this type of buck converter. This configuration is known as the discontinuous conduction mode. This region of operation may be handled by introducing an additional switching surface on the zero current axis. From the topology of the circuit, it can be seen that once the converter is in the discontinuous conduction mode, the inductor current will remain at zero while the capacitor voltage will decrease as the capacitor discharges to supply the load. Thus, once the system state trajectory intersects the zero current axis, the trajectory will remain on the zero current axis and tend toward the origin. This behavior will continue until the state trajectory hits the switching surface G and SW_1 turns on. When computing the set of reachable states in this case, it is sufficient to simply remove the set of points that fall below the zero current axis from $\mathcal{Y}(\tau)$ at the end of each computational step. If the entire set of points in $\mathcal{Y}(\tau)$ is below the zero current axis, $\mathcal{Y}(\tau)$ may simply be set equal to the point in which the switching surface G intersects the zero current axis.

TABLE II
CLOSED-LOOP BUCK CONVERTER PARAMETERS

R_L [Ω]	10e-3	V_s [V]	12
L [H]	50e-6	I_c [A]	2
C [F]	44.1e-6	I [A]	2
k_v	100	I_{ref} [A]	4
k_i	25	V_{ref} [V]	5

The closed-loop reachability problem was solved for the buck converter of Fig. 1 with parameters and switching boundary given in Table II. Figure 4 contains the steady-state solution to the closed-loop reachability problem. The set of reachable states $\mathcal{R}(t)$ for this converter in steady-state operation is the region enclosed by the blue traces and the zero current axis. The switching surface G is shown by the diagonal red line in the figure. It is apparent that the set of reachable states violates the voltage regulation requirements. Thus, the design may need to be further modified to meet this requirement. In some cases, it is possible for the system to violate the performance bounds for a short period of time without jeopardizing the functionality of the system. These types of performance bounds are known as soft bounds (e.g. bounds imposed by component thermal limits). However, there

also exist other cases in which if a certain performance bound were to be violated, the system would cease to operate. These performance bounds are known as hard bounds (e.g. a fuse that would operate if the current becomes too large).
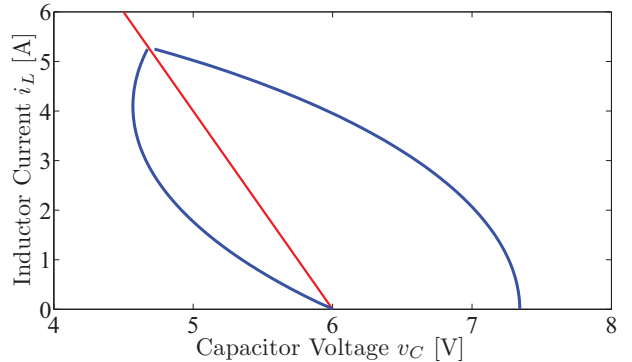

Fig. 4. Closed-loop steady-state reach set for buck converter of Table II.

IV. BOOST CONVERTER ANALYSIS

The proposed methods may be applied to any converter architecture so long as the converter operation may be accurately modeled by a linear switched state-space model and the switching function is known. In this section, the proposed method is applied to verify the design of a boost converter. Consider the boost converter of Fig. 5. The function of this converter is to produce an output dc voltage that is higher than the input dc voltage. The A and B matrices of the switched-linear dynamics of a boost converter are given by

$$A_0 = \begin{bmatrix} 0 & \frac{1}{C} \\ -\frac{1}{L} & -\frac{R_L}{L} \end{bmatrix}, \quad B_0 = \begin{bmatrix} 0 & -\frac{1}{C} \\ \frac{1}{L} & 0 \end{bmatrix}$$
$$A_1 = \begin{bmatrix} 0 & 0 \\ 0 & -\frac{R_L}{L} \end{bmatrix}, \quad B_1 = \begin{bmatrix} 0 & -\frac{1}{C} \\ \frac{1}{L} & 0 \end{bmatrix} \quad (13)$$

where $q = 1$ when SW_1 is closed and SW_2 is open and $q = 0$ when SW_1 is open and SW_2 is closed. The uncontrolled inputs to the boost converter are the source voltage V_s and the load current i_{load}.

A. Open-Loop Design Verification

Here, the open-loop verification method is applied to the boost converter shown in Fig. 5, with parameters given in Table III. The function of this converter is to step up 12V dc to 48V dc. Equation (3) describes the bounds on the converter inputs. As before, for computational purposes Ω_w is assumed to be the minimum volume ellipsoid that contains the true set of all possible inputs. The switching function for this converter is also given by (12).

Equation (5) was solved using the algorithm for open-loop verification presented Section II for $\eta_1 = [1 \ 0]'$ and $\eta_2 = [0 \ 1]'$, and a sufficiently long period of time to allow the reach set $\mathcal{R}(t)$ to come to steady-state. Figure 6 shows the steady-state open-loop reach set for the boost converter
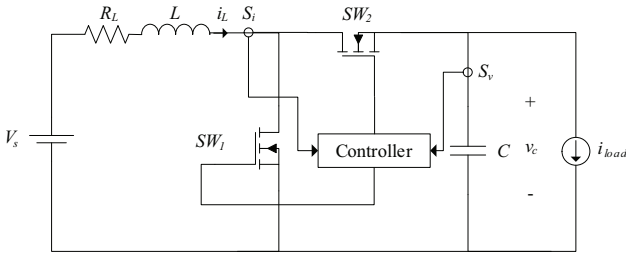
Fig. 5. Boost converter architecture.

TABLE III
OPEN-LOOP BOOST CONVERTER PARAMETERS

R_L $[\Omega]$	0.2	V_c $[V]$	12
L $[H]$	50e-6	V $[V]$	0.1
C $[F]$	20e-5	I_c $[A]$	2
f $[kHz]$	200	I $[A]$	0.25
D	0.79	λ $[\%]$	5

with parameters given in Table III. As before, two sets of ellipsoids, one for each η (η_1 in red and η_2 in blue), are shown for selected points in time during one switching period of the converter's steady-state operation. Also shown, by the dotted black traces is the output voltage tolerance as specified by the converter design requirements. The steady-state reach set of the converter is completely contained within the acceptable region.
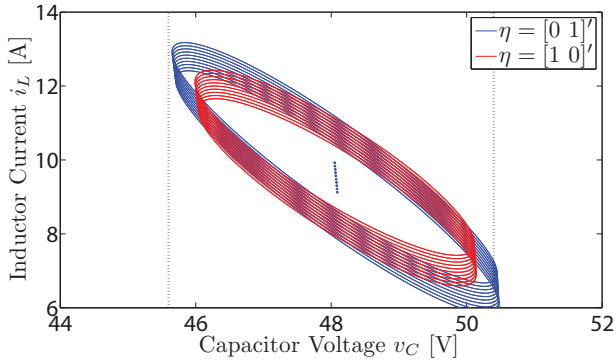

Fig. 6. Open-loop reach set for the boost converter of Table III.

B. Closed-Loop Design Verification

Here, the closed-loop verification method is considered. To illustrate the method, it is applied to a boost converter that uses a static linear switching boundary to step up 12V dc to 48V dc. A practical problem with this type of control of power electronics converters is that as the converter trajectory converges to the switching surface, the switching frequency of the converter tends to infinity. This is commonly known as switch chattering [16]. One method that can be used to mitigate switch chattering is to add a hysteresis band (or dead band) around the switching surface. For a converter with two possible configurations, the hysteresis band may

be represented in the converter state space as two separate switching boundaries G_1 and G_2. Where G_1 lies below and to the left of G_2 in the state space. The converter then operates by activating one configuration when the state trajectory is below and to the left of G_1 and then switching to the other configuration when the state trajectory is above and to the right of G_2. When the state trajectory is between the two switching boundaries the converter remains in its previous configuration. The switching function for a hysteresis-controlled converter is given by

$$\sigma(t) = \begin{cases} 0 & K'(x_{ref} - x) \leq -\Delta \\ \sigma(t - \tau) & -\Delta < K'(x_{ref} - x) \leq \Delta \\ 1 & K'(x_{ref} - x) > \Delta, \end{cases} \quad (14)$$

where $K = [k_i \ k_v]'$ and $x_{ref} = [I_{ref} \ V_{ref}]$ for the boost converter, Δ is a constant that describes the width of the hysteresis band, and τ is the time delay between successive computations of the switching function $\sigma(t)$. For simplicity, it was assumed that this time delay is zero.

TABLE IV
CLOSED-LOOP BOOST CONVERTER PARAMETERS

R_L $[\Omega]$	10e-3	V_s $[V]$	12
L $[H]$	50e-6	I_c $[A]$	2
C $[F]$	20e-6	I $[A]$	0.25
k_v	2	V_{ref} $[V]$	48
k_i	10	I_{ref} $[A]$	4.27
Δ	5	λ $[\%]$	5

The closed-loop reachability problem was solved for the boost converter with switching function given by (14) and converter parameters given in Table IV. Fig. 7 shows the reach set for both startup (a) and steady-state (b) operation. In both figures, the switching boundaries G_1 and G_2 are shown by the solid red lines and the set of reachable states $\mathcal{R}(t)$ is contained within the solid blue regions. Fig. 7(b) also shows a sample converter trajectory in green.

It can be seen in Fig. 7(a) that the boost converter with this type of control will start up by first closing SW_1 to charge the inductor. Then, once the state trajectory reaches G_2, a switch action will occur and the inductor current will be discharged into the capacitor and the load. Subsequent switch actions will occur to cause the converter state trajectory to slide down the guards to the steady-state operating region as shown in Fig 7(b). The sample converter trajectory is completely contained within the steady-state reach set $\mathcal{R}(t)$ as shown in Fig. 7(b). However, this converter design does not meet the voltage regulation design requirement.

V. CONCLUSION

In this paper, a method for design verification of power electronics systems subject to bounded uncertain inputs was proposed. The method relies on solving the reachability problem for the full switching model of such converters, whereas previous methods focused only on the linearized averaged
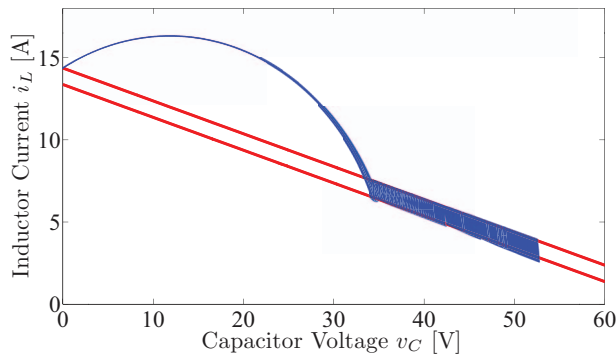
(a) Reach set during startup for hysteresis-controlled boost converter.
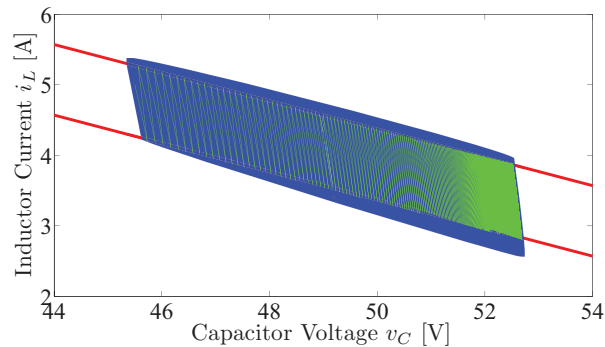
(b) Steady-state reach set for hysteresis-controlled boost converter.

Fig. 7. Closed-loop reach set for hysteresis-controlled boost converter of Table IV.

model. One of the advantages of this technique is that it provides an analytically tractable solution, which reduces the computational burden of other techniques that are based on simulating the system for every possible realization of the uncontrolled input. The analytically tractable solutions provided by the proposed method also give further insight into the influence of design parameters and control techniques on the overall system performance. In the buck and boost converter examples, it was shown that this methodology can be applied to any converter modeled as a linear switched system and any linear control.

References

[1] Intel. (2002) Intel® pentium® 4 processor vr-down design guidelines. [Online]. Available: http://download.intel.com/design/Pentium4/guides/24989104.pdf
[2] L. Kamas and S. Sanders, "Power electronic circuit reliability analysis incorporating parallel simulations," in *Proc. IEEE Workshop on Computers in Power Electronics*, August 1996, pp. 45–51.
[3] W. Huang, D. Clafette, G. Shcuelling, M. Crowther, and J. Wallace, "System accuracy analysis of multiphase voltage regulator module," *IEEE Transactions on Power Electronics*, vol. 22, no. 3, pp. 1019–1026, May 2007.
[4] A. Domínguez-García and P. Krein, "Integrating reliability into the design of fault-tolerant power electronics systems," in *Proceedings of PESC 2008*, Rhodes, Greece, 2008.
[5] A. Kurzhanski and P. Varaiya, "Ellipsoidal techniques for reachability analysis. parts I & II," *Optimization Methods and Software*, vol. 17, pp. 177–206 and 207–237, February 2000.
[6] A. Kurzhanski, I. Mitchell, and P. Varaiya, "Ellipsoidal techniques for hybrid dynamics: the reachability problem," *Optimization Theory and Applications*, vol. 128, no. 3, pp. 499–521, March 2006.
[7] F. Schweppe, *Uncertain Dynamic Systems*. Englewood Cliffs, NJ: Prentice-Hall Inc., 1973.
[8] A. Kurzhanski and I. Vályi, *Ellipsoidal Calculus for Estimation and Control*. Boston, MA: Birkhauser, 1997.
[9] F. Chernousko, "What is ellipsoidal modelling and how to use it for control and state estimation," in *Whys and Hows in Uncertainty Modelling: Probability, Fuzziness, and Anti-Optimization*, ser. CISM Courses and Lectures, I. Elishakoff, Ed. Vienna, Austria: Springer, 1999, ch. 3, pp. 127–188.
[10] A. Chutinan and B. H. Krogh, "Computing polyhedral approximations to flow pipes for dynamic systems," in *Proceedings of the 37th IEEE Conference on Decision and Control*, Tampa, FL, 1998.
[11] A. Girard, "Reachability of uncertain linear systems using zonotopes," in *Proceedings of HSCC 2005*, Zurich, Switzerland, 2005.
[12] A. Chutinan and B. H. Krogh, "Computational techniques for hybrid system verification," *IEEE Transactions on Automatic Control*, vol. 48, no. 1, pp. 64–75, Jan. 2003.
[13] E. Asarin, T. Dang, G. Frehse, A. Girard, C. LeGuernic, and O. Maler, "Recent progress in continuous and hybrid reachability analysis," in *IEEE International Symposium on Computer-Aided Control Systems Design*, Munich, Germany, 2006, pp. 1582–1587.
[14] P. Krein, *Elements of Power Electronics*. New York, NY: Oxford University Press, 1997.
[15] A. Kurzhanskiy and P. Varaiya, *Ellipsoidal Toolbox, http://www.eecs.berkeley.edu/ akurzhan/ellipsoids/ (web page and software)*, 2006.
[16] R. Munzert and P. Krein, "Issues in boundary control (of power converters)," in *Proceedings of the Power Electronics Specialists Conference*, Baveno, Italy, 1996.